ChemElectroChem

Research Article
doi.org/10.1002/celc.202200991

Chemistry Europe
European Chemical Societies Publishing

www.chemelectrochem.org

The Influence of Loadings and Substrates on the Performance of Nickel-Based Catalysts for the Oxygen Evolution Reaction

Wulyu Jiang,[a, b] Werner Lehnert,[a, b] and Meital Shviro*[a, c]

Efficient and durable catalysts for the oxygen evolution reaction (OER) are of great importance for energy storage and conversion devices. However, an objective evaluation and fair comparison of different catalysts remain challenging due to the different catalyst loadings and substrates for OER measurements. In this work, we investigated NiFe layer double hydroxide and commercial Ni/NiO catalysts with different loadings and substrates of glassy carbon (GC), porous nickel foam (NF), and carbon paper (CP). The activity, cycling stability, and potentiostatic stability of the catalysts are compared with respect to the loading and substrate. Catalyst loading exhibits a volcano trend with OER activity, while it has little impact on stability. The 3D substrates NF and CP significantly improved the OER activity of the catalysts compared to GC, especially at higher loadings. The consistent degradation trend of the catalysts confirms the validity of using NF or CP as substrates for the stability test.

Introduction

Water electrolysis, a simple technique to store clean electrical energy from solar and wind resources in the form of hydrogen gas, is expected to achieve a sustainable and critical energy landscape and infrastructure.[1] Water electrolysis consists of two half-cell reactions: the hydrogen evolution reaction (HER) at the cathode and the oxygen evolution reaction (OER) at the anode. The overall energy efficiency of water electrolysis is significantly impeded by the sluggish kinetics of the OER process.[2] To overcome the high overpotential of the OER, numerous electrocatalysts based on non-precious metals have been developed, especially nickel-based catalysts due to their dominant catalytic performance and economic requirements.[2–5] The key to successfully identifying the optimal catalyst is to evaluate the catalytical properties of a particular catalyst.

[a] W. Jiang, Prof. Dr. W. Lehnert, Dr. M. Shviro
Forschungszentrum Jülich GmbH
Institute of Energy and Climate Research
Electrochemical Process Engineering (IEK-14)
52425 Jülich, Germany
[b] W. Jiang, Prof. Dr. W. Lehnert
Faculty of Mechanical Engineering
RWTH Aachen University
52056 Aachen, Germany
[c] Dr. M. Shviro
Present address:
Chemistry and Nanoscience Center
National Renewable Energy Laboratory (NREL)
Golden, CO, 80401, United States
E-mail: meital.shviro@nrel.gov

Supporting information for this article is available on the WWW under https://doi.org/10.1002/celc.202200991

However, objective evaluation of OER catalysts is hindered by the lack of standardization in both measurement and reporting of electrocatalytic data.[6,7] Catalyst loadings are regarded to be strongly related to their activities towards the OER, and several research groups have reported a loading-dependent activity of nickel-based OER catalysts.[8] In general, representative polarization curves of a certain catalyst with several different loadings were compared and the one with the highest current density was selected to demonstrate the nominal activity of the catalyst.[9,10] This led to a huge difference in the catalyst loadings reported by various research groups, ranging from 0.1 to over 4 mg cm^{-2}, as summarized in Table S1, bringing constraints on fair comparison of catalyst activity. Therefore, a more systematic and quantitative comparison of the effects on the OER properties, including activity and stability, is critical but absent. At the same time, typical OER catalysts are deposited on a variety of different substrates, making it challenging to compare the activity and stability of these different electrodes. It is known that the OER current density depends largely on the supporting substrates. According to previous guidelines, nanoengineering electrodes can increase the surface area to expose more active sites than the flat glassy carbon (GC) electrode.[8] While it is also common in the literature that research groups test their catalysts in different porous 3D electrodes, for example, nickel foam (NF) and carbon paper (CP), as listed in Table S1. Moreover, their potential impact on the stability performance of catalysts is rarely studied before. Therefore, objective comparisons between OER catalysts are blurred by the use of different supports and loadings. Hence, the adoption of standard test protocols for the evaluation of OER catalysts is recommended.

Here, we selected two typical OER catalysts, commercial nickel oxide nanoparticles (referred to as Ni/NiO), and synthesized highly active NiFe layered double hydroxides (referred to as NiFe LDH). A standardized protocol was developed to

compare the catalysts on different conductive supports and loadings in terms of activity and stability. A quantitative relationship between catalyst loading and OER activity is clear. The superior properties of porous supports on nickel-based catalysts are also investigated by electrochemical comparisons and structural observations. This work highlights the role of the working electrode, particularly the substrates and the amount of catalyst cast, in the evaluation of catalysts.

Results and discussion

In the present study, we aim to investigate the influence of loadings and substrates of catalysts on their OER properties. Here we choose two typical samples as OER catalysts, the commercial Ni/NiO nanoparticles with ordinary catalytic activity and synthesized NiFe LDH with excellent OER performance. As substrates, we chose the common GC, NF and CP as conducting supports for comparison.

Loading effect on OER performance

To maximize the catalytic properties, several catalyst loadings were usually tried and compared, and finally, the optimum loading was selected that exhibited the best nominal activity of a given catalyst. Thus, it is known that the amount of catalyst used for the half-cell measurement affects the current density shown, but the reasons and magnitude of this are not clear. At the same time, it is unclear whether this also affects the evaluation of stability, the other crucial parameter for catalysts.

Loading effect on the activities of catalysts

Therefore, the influence of added catalyst loading on their activities is investigated at different substrates, and firstly common GC electrode (used for rotating disk electrode (RDE) tests). Due to the relatively small geometric area of the GC electrode (0.196 cm^2), the catalyst loading on GC is usually low, ranging from 0.1 to 0.5 mg cm^{-2}, with 0.2 mg cm^{-2} being the most typical.[11–14] Hence, we drop cast NiFe LDH catalysts on GC with three different loadings varying from 0.2 to 0.8 mg cm^{-2} and compare their OER performance shown in Figure 1. When the loading is increased from 0.2 to 0.4 mg cm^{-2}, the NiFe LDH electrode show higher current density and lower overpotential at 50 mA cm^{-2} (Figure 1a and 1b), indicating better OER activity. Then, more catalysts are added to reach 0.8 mg cm^{-2}, and both the polarization curve and the overpotential show a decrease in activity. In other words, moderate loading of catalysts on GC showed the best OER activity, while low or high loading would lead to decreased performance. This trend is also consistent with the results of other catalysts in previous work.[9,10]

To clarify the underlying reason, we compare their Tafel slope and electrochemical surface area (ECSA, details in the experimental section) (Figures 1c and 1d). In the low current density range controlled by transport-free reaction kinetics, the NiFe LDH electrode from 0.2 to 0.4 mg cm^{-2}, shows a decreased Tafel slope from 60 to 43 mV dec^{-1} and an increased ECSA from 7.48 to 9.03 μF cm^{-2}, indicating a more active site and faster kinetics favoring the transport and separation of the resulting charge and mass carriers. Further increasing the catalysts loading to 0.8 mg cm^{-2} results in a lower ECSA, because the GC is a 2D electrode, the surface area is fixed at 0.196 cm^2, higher

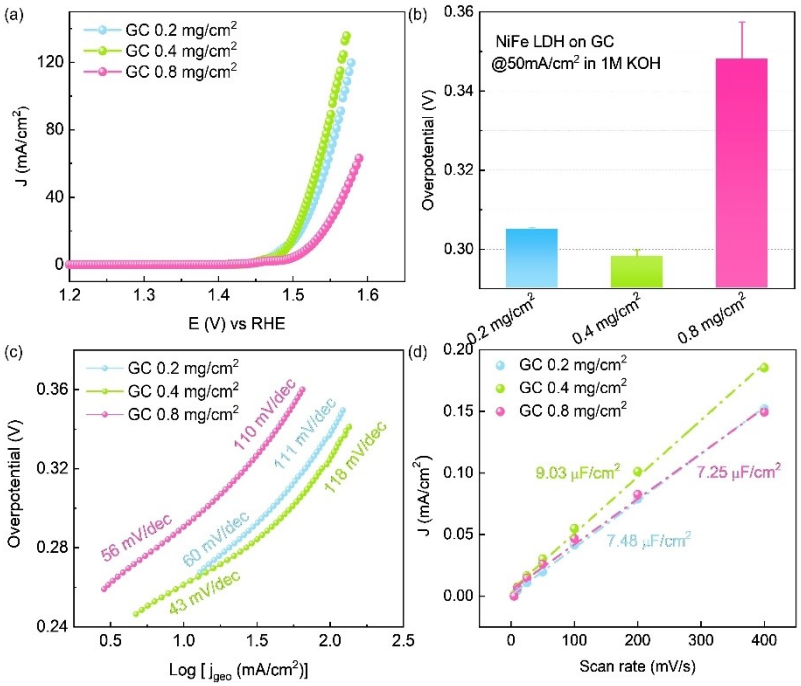

Figure 1. Loading effect of NiFe LDH catalysts on GC electrode. (a) OER polarization curves, corresponding (b) overpotentials at 50 mA cm^{-2}, (c) Tafel slopes and (d) ECSA of the NiFe LDH catalysts with various loading 0.2, 0.4 and 0.8 mg cm^{-2} in 1 M KOH.

loadings would probably lead to the mutual coverage and overlap of NiFe LDH nanosheets. At the same time, the thicker coated catalyst layer on GC would increase the resistance of electron transfer between catalysts and substrates,[3] therefore, the Tafel slope at 0.8 mg cm^{-2} is also increased compared with the value at 0.4 mg cm^{-2}. While the similar raised Tafel slopes (110-120 mV/dec) at high current density indicate their rate limiting step changes due to the increased resistance of ions, electrons, and oxygen transport, consistent with previous studies.[15,16]

Besides of the synthesized NiFe LDH catalysts, we also confirm the loading effect on GC electrode for commercial Ni/NiO powders (Figure S1). Similarly, as the loading increase gradually from 0.2 to 0.8 mg cm^{-2}, the corresponding Ni oxidation peak and ECSA enlarge simultaneously, indicating more Ni/NiO catalysts participate in the reaction. However, the highest activity plateau is obtained at 0.4 mg cm^{-2}, and the lower current density for 0.8 mg cm^{-2} Ni/NiO at high potential is limited by mass transfer process.

To reduce catalyst loading and increase catalytic activity, nanostructure electrodes in combination with large surface area substrates are often used, for example, catalysts coated on nickel or carbon supports. Therefore, the effect of catalyst loading on OER activity is studied when using CP and NF as substrates. Figures 2a–c show the structure of NiFe LDH catalysts coated on CP with various loading 0.2, 0.4, and 0.8 mg cm^{-2}. The three-dimensional composite electrode structure supported by carbon fiber provide plenty of space for catalysts, hence, as the loading of NiFe LDH increase, the distributed catalysts on the fiber surface also gradually expand. The corresponding catalyst morphology revealed by higher magnification SEM images on a single fiber (Figure S2a and S2b) confirm not only more catalysts are coated on carbon substrates as the loading increase from 0.2 to 0.8 mg cm^{-2}, but also a certain amount of local agglomeration of catalysts, this is the reason why the active site number and catalytical activity are not rising as loading in parallel. This phenomenon is confirmed by their catalytic performance in Figures 2d and 2e. Their OER activities improve as the loading of NiFe LDH increase from 0.2 to 0.8 mg cm^{-2} and reach a plateau at 1.2 mg cm^{-2}. At the same time, the gradually increasing nickel oxidation peak and the consequent weakening carbon oxidation peak in Figure 2f also verify the dominating role of catalyst itself and less involvement and influence from the CP substrate as more catalysts load.

To further reveal the impact from catalyst loading on the number of participated metal sites, the pre-OER nickel redox peaks are analyzed. Since the contribution from CP and NF cannot be excluded, the former mentioned ECSA measurement from double layer capacitance method would lead to an overestimation of catalyst sites. Another electrochemical method, the redox peak analysis, though has its own limitations, for instance, uncertain specific charge, unclear number of transfer electron and so on, however, is still available complementary to compare the general active site trends.[17–19] Therefore, the nickel redox peak in the cyclic voltammetry (CV) curves of NiFe LDH on CP are presented in Figure S3a, and the corresponding peak intensity, integral peak area, and OER currents are compared at each loading to roughly evaluate their intrinsic activities in Figure S3b. The consistently increasing trend of the intensity and area of reduction peak from 0.2 to 0.8 mg/cm^2 NiFe LDH indicate more nickel sites at higher loadings, accounting for the promoted OER current densities. The fact that the current density at 1.2 mg/cm^2 does not increase further with more Ni sites may be limited by the mass transfer process. Therefore, the high current density of NiFe LDH catalysts with increased loading from 0.2 to 0.8 mg/cm^2 come from more involved active sites, with actually similar intrinsic activity of

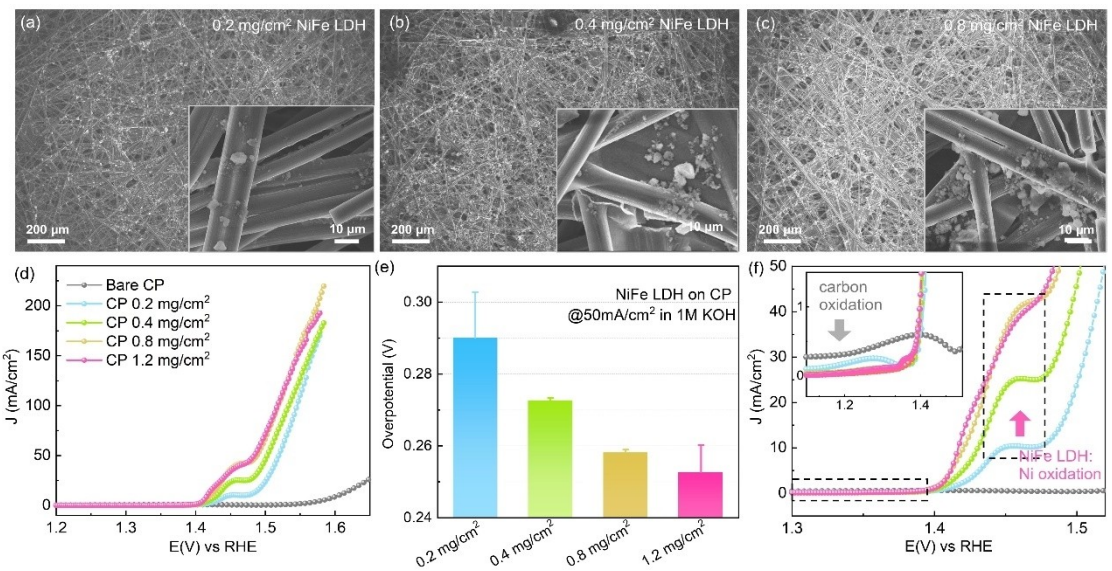

Figure 2. Loading effect of NiFe LDH catalysts on CP. (a-c) SEM images of NiFe LDH catalysts with various loading 0.2, 0.4 and 0.8 mg cm^{-2} on CP; (d) polarization curve, (e) corresponding overpotential at 50 mA cm^{-2} and (f) magnification of carbon and nickel oxidation range from 1.3–1.5 V from (d) of NiFe LDH catalysts with various loading 0.2, 0.4, 0.8 and 1.2 mg cm^{-2} in 1 M KOH.

these sites, whereas a further higher loading even exhibits lower intrinsic activity.

In addition, the effect of catalyst loading on NF shows similar trends: SEM images in Figures 3a-c and Figure S2c–d indicate more NiFe LDH catalysts are gradually coated on the NF surface with increasing loading. The electrochemical behaviors in Figures 3d-f demonstrate NF are partly covered by catalysts when firstly coating 0.2 mg cm^{-2} NiFe LDH, with increased OER current, reduced overpotential and weakened nickel oxidation from NF. Then the loading increase from 0.2 to 0.4 mg cm^{-2}, and more catalysts cover the substrate and participate in the OER process with more notable activity. Further increase of loading to 0.8 mg cm^{-2} does not give higher activity together with the almost unchanged nickel oxidation peaks from NF substrate and NiFe LDH catalysts. This conclusion is also in agreement with the trend reported in the literature.[20]

In addition to the synthesized NiFe LDH catalysts, the OER activities of the commercial Ni/NiO powders are compared on NF and CP with different loadings (Figure S4). Consistently, the area of the associated nickel oxidation peak increases with larger loadings, but the corresponding OER activity does not increase indefinitely. Based on the above results, catalyst loading exhibits an unignorable effect on the activity: in a certain range, increased loading would lead to a higher current density due to the involvement of more active sites in the reaction, but a further increase in loading does not bring a sustained enhancement in activity, due to the catalyst intercoverage and mass transfer at large current densities. Also, this effect is more pronounced for the highly active NiFe LDH catalysts while the difference in activity for different loadings is relatively slight for common Ni/NiO catalysts.

Loading effect on cycling stability of OER catalysts

Stability is another critical merit when selecting OER catalysts for applications as practical water electrolyzers have to operate consistently and efficiently over a long time (over thousands of hours or cycles). Therefore, it is also essential to consider the effect of loadings on catalyst stability performance. There are two common strategies used for stability measurements: cycling the electrode and keeping the electrode at galvanostatic or potentiostatic conditions, simulating their respective situations for practical applications.[8]

The cycling stability of NiFe LDH catalysts is measured with different loadings of 0.2, 0.4, and 0.8 mg cm^{-2} by comparing their polarization curves before and after 1000 cycles between 1.0-1.7 V in 1 M KOH. As shown in Figures 4a and 4d, all the NiFe LDHs on the GC electrode show reduced current densities and increased overpotentials, indicating degraded performance during the cycling process. The more significant degradation at 0.8 mg cm^{-2} may be due to low conductivity and mass transfer limitations at high loading, as discussed in the Pt/C system.[7] Similarly, NiFe LDH catalysts with different loadings on NF and CP (Figures 4b–4f) exhibit a comparable stability trend, and a certain degree of decline. The low current density of bare NF and CP during the same process confirms the dominant role of catalysts in electrode performance, not substrates. Equivalent experiments are also conducted in the Ni/NiO catalysts with different loadings (Figure S4), which exhibit a certain degree of activity improvement for all three kinds of substrates regardless of the loading. Namely, the catalyst loading does not affect its performance in terms of cycling stability trend, although the degree of changes may vary slightly.

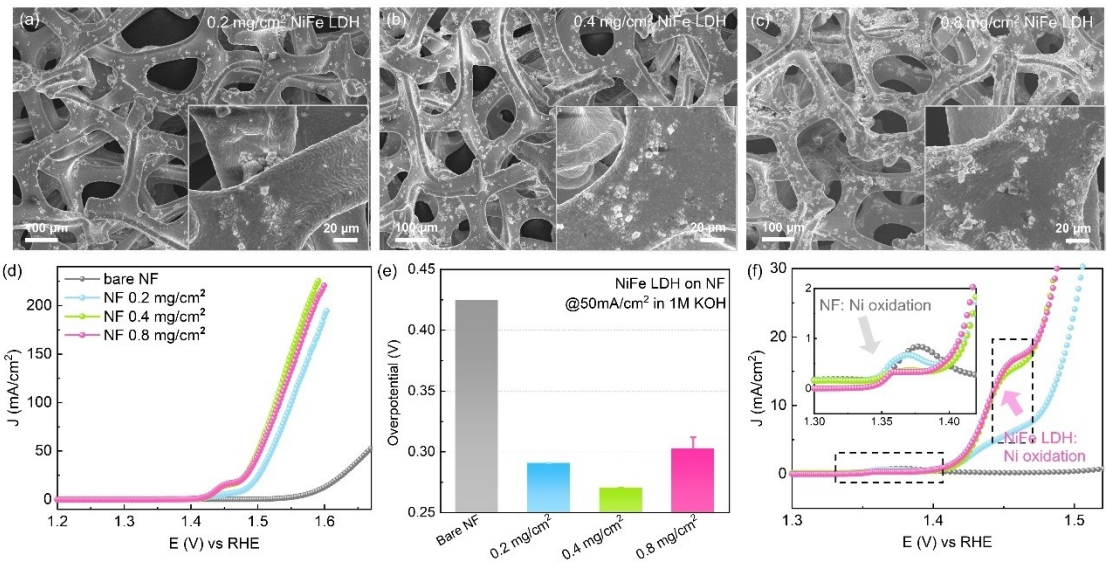

Figure 3. Loading effect of NiFe LDH catalyst on NF. (a-c) SEM images of NiFe LDH catalysts with various loading 0.2, 0.4 and 0.8 mg cm^{-2} on NF; corresponding (d) polarization curve, (e) overpotentials at 50 mA cm^{-2} and (f) magnification of nickel oxidation range from 1.3–1.5 V from (d) of these NiFe LDH catalysts in 1 M KOH.

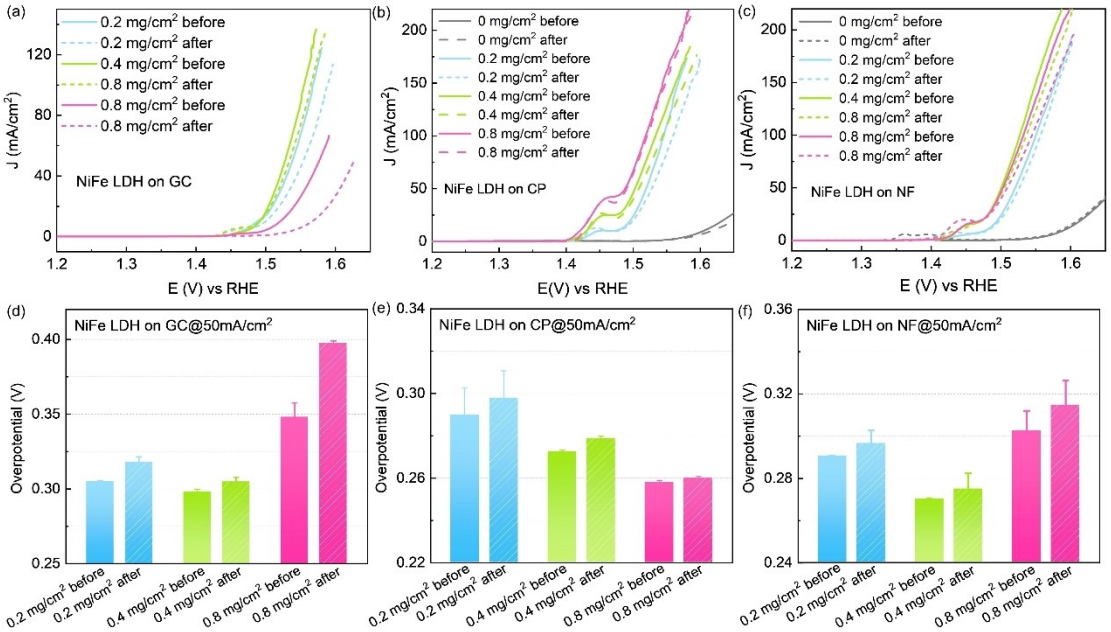

Figure 4. Loading effect on the cycling stability of NiFe LDH catalysts. (a-c) OER polarization curves and (d-f) corresponding overpotentials at 50 mA cm^{-2} of the NiFe LDH catalysts with different loadings 0.2, 0.4 and 0.8 mg cm^{-2} on various substrates before and after cycling between 1.0–1.7 V for 1000 cycles in 1 M KOH. NiFe LDH on (a,d) GC, (b,e) CP and (c,f) NF. The bare CP and NF was used for comparison in Figure 4b and 4c.

Loading effect on potentiostatic stability of OER catalysts

Subsequently, the possible affinity between catalyst loading and potentiostatic stabilities is also investigated. As shown in Figure 5, the polarization curves and corresponding overpotentials of NiFe LDH catalysts with two loadings on a given substrate are recorded before and after holding at 1.6 V for 20 hours. The catalysts on each substrate GC, CP or NF show some decrease in current density and increase in overpotential, indicating the same stability trend for different loadings at 0.2 and 0.8 mg cm^{-2}. This conclusion can also be confirmed from the identical experiments in the Ni/NiO system with different

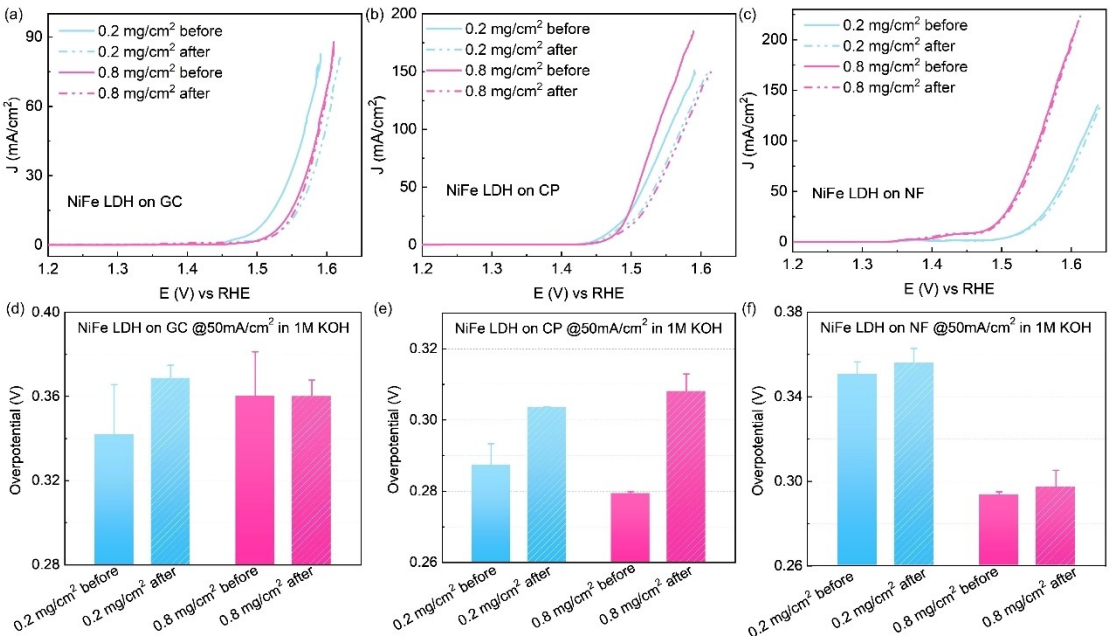

Figure 5. Loading effect on the potentiostatic stability of NiFe LDH catalysts. (a-c) OER polarization curves and (d-f) corresponding overpotentials at 50 mA cm^{-2} of the NiFe LDH catalysts on various substrates before and after keeping at 1.6 V for 20 h in 1 M KOH solution. NiFe LDH on (a,d) GC, (b,e) CP and (c,f) NF.

loadings but a similar increase in activity after the aging process with constant potential (Figure S5). This means that loading also does not change the potentiostatic stability of the catalysts.

Substrate effect on OER performance

The effect of loading on the performance of the catalyst was shown in the previous section, but the substrate, which serves as a current collector and mass carrier, to which OER is very sensitive, is not always the same in the test protocols. Among them, CP and NF are suitable candidates for catalyst support in addition to GC due to their low cost, excellent conductivity, mechanical strength, and chemical stability under alkaline conditions.[21–24] Thus, an objective evaluation of OER catalysts would be blurred by the different substrates. The formerly-presented OER performance of NiFe LDH and Ni/NiO in the three kinds of substrates have exhibited noticeable distinctions, though not specifically stated. Therefore, in this section, the performance of NiFe LDH catalysts on GC, CP, and NF is compared directly then the possible effects of the substrates on OER activity and stability could be visualized more clearly.

Substrate effect on the activities of catalysts

The structures of NiFe LDH catalysts on various substrates are observed by SEM images, as shown in Figures 6a–c, the hierarchical structure was assembled from massive NiFe LDH nanosheets, connecting to adjacent ones and covering each other. While they are more dispersed on the surface of the NF and CP supports. Consequently, such electrodes would have a larger active area, which was confirmed by the higher nickel oxidation peaks when NiFe LDHs are coated on NF and CP compared with their counterparts on GC (Figures 6d and 6f). Their corresponding current densities and overpotentials also state the substrate effect on the OER activities: NiFe LDH/CP > NiFe LDH/NF > NiFe LDH/GC. This trend is more obvious at 0.8 mg cm^{-2} NiFe LDH (Figures 6d-g), owing to the more crucial role of catalyst distribution at high loadings.

To identify the specific role of different substrates, the pre-OER nickel redox peaks in their corresponding CV curves are analyzed in Figure S6. The tiny redox peak of bare NF indicates its ignorable contribution when using NF as support and the dominance from NiFe LDH catalysts. At 0.2 mg/cm^2, NF and CP exhibit much higher peak intensity and area than GC, indicating more active sites as expected from the SEM images of the 3D electrode. However, the mismatched increase in current densities indicates their different intrinsic OER activities. NiFe LDH on GC is better than that on NF and CP, because of its accelerated mass transfer with the rotation of RDE. While at higher loading of 0.8 mg/cm^2, the thickened catalyst layer on GC would restrict mass/charge transfer, leading to reduced intrinsic activity. For NF and CP, further enlarged surface area confirms their superior effect to exposing active sites as substrates. At the same time, it is worthwhile to note the NiFe LDH on NF shows improved intrinsic activity than that on CP, especially at high loadings, which emphasizes the special features of nickel-based substrates as reported in other catalysts.[19,25]

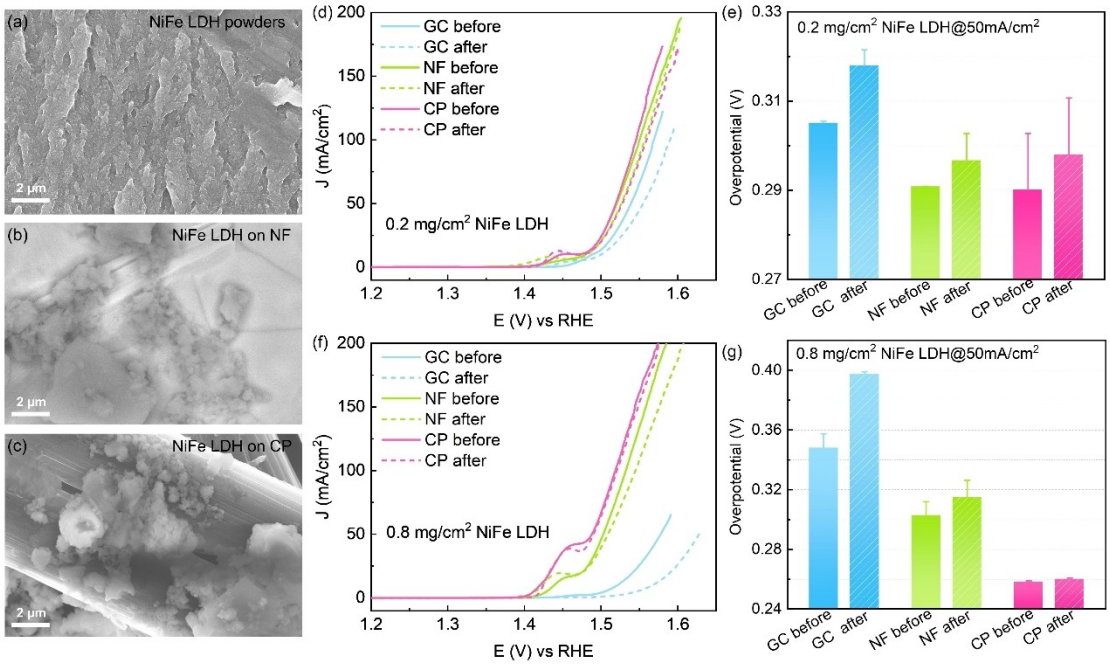

Figure 6. (a-c) SEM images of the NiFe LDH catalysts on various substrates. (a) initial NiFe LDH powders, NiFe LDH on (b) NF and (c) CP. The corresponding (d,f) OER polarization curves and (e,g) overpotentials at 50 mA cm^{-2} before and after cycling between 1.0–1.7 V for 1000 cycles in 1 M KOH. Among them, the loading of NiFe LDH catalysts is (d,e) 0.2 mg cm^{-2} and (f,g) 0.8 mg cm^{-2} .

Such substrate effect has also been studied for Ni/NiO catalysts. As shown in Figure S7, Ni/NiO on porous 3D NF and CP supports show higher current density and lower overpotential compared to Ni/NiO on GC for 0.2 and 0.8 mg cm^{-2}. Although the substrate effect is weaker due to the low intrinsic activity of Ni/NiO catalysts compared to NiFe LDH, it can be assumed that the influence of the substrate is crucial for most of the reported highly active catalysts. However, previous literature has often coated catalysts with high loadings on substrates other than GC for half-cell testing, for example, over 1 to 4 mg cm^{-2} catalysts on NF or CP, which might overestimate the OER performance.[26–30] Our results show that the substrates contribute significantly to the nominal activities of the catalysts, especially at high loadings, therefore these conditions need to be carefully considered to give a fair evaluation of the activity of different catalysts.

Substrate effect on cycling stability of catalysts

Besides the activity, the OER stability of catalysts is often evaluated on other substrates, for instance, NF or CP, not conventional GC, therefore, it is necessary to figure out whether these different substrates would affect the stability performance of catalysts. As shown in Figures 6d–g, 0.2 and 0.8 mg cm^{-2} NiFe LDH catalysts on GC, NF, and CP all exhibit reduced current density and increased overpotential after 1000 cycles, while a slight difference in their degradation degree which might come from the distinct involved active site numbers owing to the substrates. At the same time, the counterpart experiments of Ni/NiO catalysts in Figure S7 show the same stability trend on different supports as well. In general, the supports do not change the OER stability trend of the loaded catalysts.

Substrate effect on potentiostatic stability of catalysts

Compared with cycling stability, where the electrode's cycle in an oxidation/reduction process between high and low potentials, potentiostatic stability of OER catalysts implies continuous oxygen evolution process at constant high potential. Therefore, it can be inferred that the mass transfer and gas diffusion during potentiostatic conditions therein may be influenced more by the substrate of the electrode. Figure 7 illustrates a comparison of the stability of the NiFe LDH catalysts in different supports for both 0.2 and 0.8 mg cm^{-2} loadings, the polarization curves and overpotentials indicating a consistent trend of stability, the degradation before and after holding at 1.6 V for 20 hours. Such similar results, roughly comparable activation was also observed for all the Ni/NiO catalysts coated on GC, NF, and CP after the same treatment process (Figure S8). Therefore, the present results indicate that different substrates (at least NF and CP) can be used for stability testing of catalysts.[9]

However, it is worth noting that the potentiostatic stability of catalysts on GC is not always easy to achieve, as the coated electrode sometimes exhibits a significant current drop and an obvious catalyst drop is observed after maintaining the potential for a certain period.[31,32] For the OER process, the oxygen bubble continuously produced by the catalytic layer at high potential loosens the catalyst film and reduces the bonding within or with the substrate, which eventually causes some of the catalysts to fall off the GC electrode. In contrast, the porous 3D structures of NF and CP are more conducive to gas diffusion and transport, so there is almost no obvious catalyst drop-off. This might be the reason why NF or CP was mostly chosen instead of GC for potentiostatic stability tests.[9]

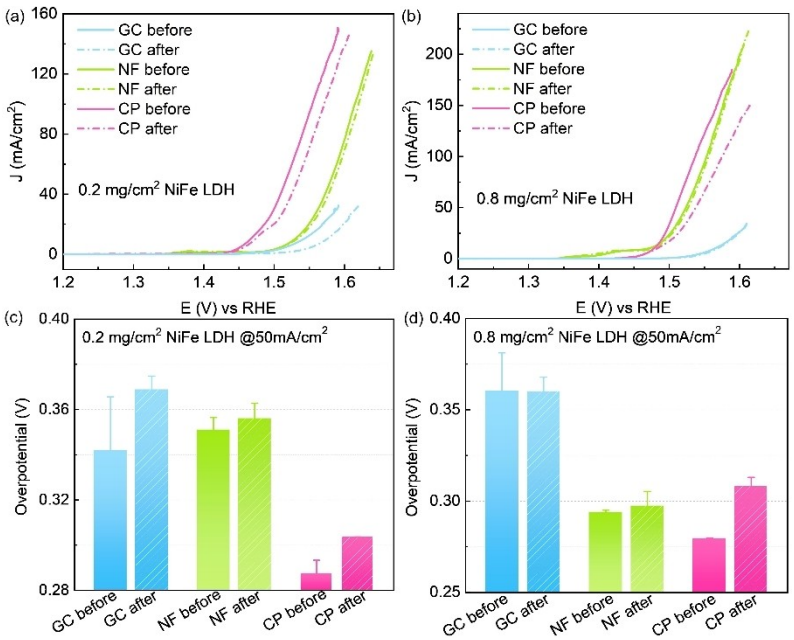

Figure 7. (a–b) OER polarization curves, and (c,d) overpotentials at 50 mA cm^{-2} of the NiFe LDH catalysts on various substrates before and after keeping at 1.6 V for 20 h in 1 M KOH solution. Among them, the loading of NiFe LDH is (a,c) 0.2 mg cm^{-2} and (b,d) 0.8 mg cm^{-2}.

Conclusion

A series of loadings, three types of substrates GC, NF, and CP, and two types of catalysts, NiFe LDH and Ni/NiO were tested for the OER to understand the effects of loading and support on activity, cycling stability, and potentiostatic stability. The ECSA of the catalysts increased with increasing loading, but the activity reached a plateau at optimum loading and then decreased due to mass transfer resistance, ohmic resistance, etc. Meanwhile, the catalyst substrates showed a dramatic influence on the OER activities, especially at high loading or high-efficiency catalysts. More catalysts on porous NF and CP substrates would expose additional active sites, while high-efficiency catalysts would enhance this effect. Thus, when reporting the activity of a novel catalyst or making comparisons with previously known catalysts, we need to pay attention to the two factors of loading and substrate and keep them consistent during the experiments. In contrast, neither loading nor substrate showed any change in the catalyst stability trend, including cycling stability and potentiostatic stability. This proves the reliability of the stability tests with supports other than GC in the literature. Moreover, the use of NF and GC is a good alternative for potentiostatic stability considering the difficulty of catalysts falling off GC. This work contributes to understanding the influence of loading and substrate on the performance of OER catalyst, guides the experimental measurement of catalyst performance, and provides objective and reasonable comparisons for mechanism research.

Experimental Section

Chemicals and Materials

Commercial nickel powder is purchased from Alfa Aesar™ (99.9% (metals basis), APS 5–20 nm, with a NiO layer of 0.5 to 1.5 nm, used as received and referred as Ni/NiO.

The NiFe LDH catalyst was synthesized by the precipitation method described in our previous work.[33] 3 mmol $Ni(NO_3)_2$ (nickel(II) nitrate hexahydrate) and 0.75 mmol $Fe(NO_3)_3$ (iron(II) nitrate hexahydrate) were added to an aqueous NaOH solution (0.15 mol/L) and stirred at 1000 rpm for 10 minutes at room temperature. Then the precipitate was washed with water and centrifuged, followed by ultrasonication for half an hour to achieve exfoliation. Finally, NiFe LDH powders were obtained by washing, centrifugation and drying.

Instrument and Methods

Electrochemical Characterization

The electrochemical performance of the catalysts was measured on an electrochemical workstation (BioLogic Scientific Instruments, SP-150) and a RDE (Pine Research Instruments) using a standard three-electrode system. A platinum wire and a Hg/HgO reference electrode (CHI, Inc.) are used as the counter electrode and reference electrode, respectively. The working electrode of GC ($\Phi = 5$ mm, Pine Research) was prepared by depositing catalyst ink with specific loadings and air-dried at room temperature for 30 minutes. The same procedure was used for NF and CP, limiting the size to 1 cm^2.

Ink preparation: 8 mg catalyst powder was mixed in a solution consisting of 1.5 mL isopropanol, 0.5 mL deionized water, and 20 μL of Nafion (5 wt%, Sigma Aldrich), and then sonicated for 40 min to get an evenly dispersed ink. All electrochemical measurements were performed in argon saturated 1 M KOH electrolyte, followed by purification with O2 for 20 min before OER experiments. The rotation speed of RDE is kept at 1600 rpm to promote the mass transfer process.

Electrochemical testing procedures: Before the activity evaluation, an activation step was conducted by cycling the electrode over the potential range of 1.0 to 1.7 V 10 times at a sweep rate of 100 mV/s. Then LSV polarization curve was performed between 1.0 V and 1.7 V vs. RHE at a sweep rate of 5 mV/s. Potentials applied were later extracted manually by the ohmic resistance (iR) drop recorded at the high-frequency region from electrochemical impedance spectroscopy experiments in the frequency range of 0.01 to10^5 Hz at 1.6 V. Cycling stability was evaluated by comparing the LSV curves before and after 1000 cycles at a scan rate of 100 mV/s in the range of 1.0–1.7 V. The chronoamperometric stability was measured by comparing the LSV curves before and after keeping the electrode at a constant potential (1.6 V vs. RHE) for a long period of 20 hours. To determine the ECSA, a series of CV curves were recorded between 1.1 to 1.2 V at various scan rates from 5, 10, 25, 50, 100, 200, to 400 mV/s in 1 M KOH. Then the capacitances were calculated from the slope of the linear relationship between current density and scan rate. In addition, we performed at least three replicate measurements for one individual experiment and then presented the averaged curve with the error bars in all figures to reduce experimental chance errors.

Physical Characterization

The morphology and structure of different electrodes were characterized by scanning electron microscopy (SEM, Zeiss Gemini Ultra Plus instrument).

Acknowledgements

This work was partially funded by the Fuel Cells and Hydrogen 2 Joint Undertaking under grant agreement No 875088. This Joint undertaking receives support from the European Union's Horizon 2020 research innovation programme and Hydrogen Europe and Hydrogen Europe Research. The authors acknowledge Ms. Schumacher Birgit for experimental support.

Conflict of Interest

The authors declare no conflict of interest.

Data Availability Statement

The data that support the findings of this study are available from the corresponding author upon reasonable request.

Keywords: electrocatalysis · loading effect · nickel-based catalysts · oxygen evolution reaction · substrates

[1] Z. Yu, Y. Duan, X. Feng, X. Yu, M. Gao, S. Yu, *Adv. Mater.* **2021**, *2007100*, 1.
[2] N. T. Suen, S. F. Hung, Q. Quan, N. Zhang, Y. J. Xu, H. M. Chen, *Chem. Soc. Rev.* **2017**, *46*, 337.
[3] F. M. Sapountzi, J. M. Gracia, C. J. Weststrate, H. O. A. Fredriksson, J. W. Niemantsverdriet, *Prog. Energy Combust. Sci.* **2017**, *58*, 1.
[4] Z. Wu, X. F. Lu, S. Zang, X. W. Lou, *Adv. Funct. Mater.* **2020**, *30*, 1910274.
[5] L. Xia, W. Jiang, H. Hartmann, J. Mayer, W. Lehnert, M. Shviro, *ACS Appl. Mater. Interfaces* **2022**, *14*, 19397.
[6] S. Anantharaj, S. R. Ede, K. Karthick, S. Sam Sankar, K. Sangeetha, P. E. Karthik, S. Kundu, *Energy Environ. Sci.* **2018**, *11*, 744.
[7] C. Wei, R. R. Rao, J. Peng, B. Huang, I. E. L. Stephens, M. Risch, Z. J. Xu, Y. Shao-Horn, *Adv. Mater.* **2019**, *31*, e1806296.
[8] D. Voiry, M. Chhowalla, Y. Gogotsi, N. A. Kotov, Y. Li, R. M. Penner, R. E. Schaak, P. S. Weiss, *ACS Nano* **2018**, *12*, 9635.
[9] C. Dong, T. Kou, H. Gao, Z. Peng, Z. Zhang, *Adv. Energy Mater.* **2018**, *8*, 1701347.
[10] M. Qian, X. Liu, S. Cui, H. Jia, P. Du, *Electrochim. Acta* **2018**, *263*, 318.
[11] J. Nai, Y. Lu, L. Yu, X. Wang, X. W. D. Lou, *Adv. Mater.* **2017**, *29*, 1703870.
[12] T. Sun, L. Xu, Y. Yan, A. A. Zakhidov, R. H. Baughman, J. Chen, *ACS Catal.* **2016**, *6*, 1446.
[13] M. Tavakkoli, M. Nosek, J. Sainio, F. Davodi, T. Kallio, P. M. Joensuu, K. Laasonen, *ACS Catal.* **2017**, *7*, 8033.
[14] B. Song, K. Li, Y. Yin, T. Wu, L. Dang, M. Cabán-Acevedo, J. Han, T. Gao, X. Wang, Z. Zhang, J. R. Schmidt, P. Xu, S. Jin, *ACS Catal.* **2017**, *7*, 8549.
[15] G. F. Li, D. Yang, P. Y. Abel Chuang, *ACS Catal.* **2018**, *8*, 11688.
[16] T. Shinagawa, A. T. Garcia-Esparza, K. Takanabe, *Sci. Rep.* **2015**, *5*.
[17] M. B. Stevens, L. J. Enman, A. S. Batchellor, M. R. Cosby, A. E. Vise, C. D. M. Trang, S. W. Boettcher, *Chem. Mater.* **2017**, *29*, 120.
[18] C. Wei, S. Sun, D. Mandler, X. Wang, S. Z. Qiao, Z. J. Xu, *Chem. Soc. Rev.* **2019**, *48*, 2518.
[19] A. Peugeot, C. E. Creissen, D. Karapinar, H. N. Tran, M. Schreiber, M. Fontecave, *Joule* **2021**, *5*, 1281.
[20] S. Cui, X. Liu, Z. Sun, P. Du, *ACS Sustainable Chem. Eng.* **2016**, *4*, 2593.
[21] B. You, Y. Sun, *Adv. Energy Mater.* **2016**, *6*, 1502333.
[22] K. Liu, F. Wang, P. He, T. A. Shifa, Z. Wang, Z. Cheng, X. Zhan, J. He, *Adv. Energy Mater.* **2018**, *8*, 1703290.
[23] S.-H. Bae, J.-E. Kim, H. Randriamahazaka, S.-Y. Moon, J.-Y. Park, I.-K. Oh, *Adv. Energy Mater.* **2017**, *7*, 1601492.
[24] P. Zhang, L. Li, D. Nordlund, H. Chen, L. Fan, B. Zhang, X. Sheng, Q. Daniel, L. Sun, *Nat. Commun.* **2018**, *9*, 381.
[25] Z. Yin, R. He, Y. Zhang, L. Feng, X. Wu, T. Wågberg, G. Hu, *J. Energy Chem.* **2022**, *69*, 585.
[26] D. Zhong, L. Zhang, C. Li, D. Li, C. Wei, Q. Zhao, J. Li, J. Gong, *J. Mater. Chem. A* **2018**, *6*, 16810.
[27] M. Qian, S. Cui, D. Jiang, L. Zhang, P. Du, *Adv. Mater.* **2017**, *29*, 1704075.
[28] L. Yu, H. Zhou, J. Sun, I. K. Mishra, D. Luo, F. Yu, Y. Yu, S. Chen, Z. Ren, *J. Mater. Chem. A* **2018**, *6*, 13619.
[29] E. Hu, Y. Feng, J. Nai, D. Zhao, Y. Hu, X. W. Lou, *Energy Environ. Sci.* **2018**, *11*, 872.
[30] H. J. Song, H. Yoon, B. Ju, G.-H. Lee, D.-W. Kim, *Adv. Energy Mater.* **2018**, *8*, 1802319.
[31] Y. Shi, Y. Xu, S. Zhuo, J. Zhang, B. Zhang, *ACS Appl. Mater. Interfaces* **2015**, *7*, 2376.
[32] C. Song, G. Wang, B. Li, C. Miao, K. Ma, K. Zhu, K. Cheng, K. Ye, J. Yan, D. Cao, J. Yin, *Electrochim. Acta* **2019**, *299*, 395.
[33] W. Jiang, A. Y. Faid, B. F. Gomes, I. Galkina, L. Xia, C. M. S. L. M. Desmau, P. Borowski, H. Hartmann, A. Maljusch, A. Besmehn, C. Roth, S. Sunde, W. Lehnert, M. Shviro, *Adv. Funct. Mater.* **2022**, *2203520*.

Manuscript received: September 27, 2022
Revised manuscript received: November 10, 2022